Physics Letters A ••• (••••) •••–•••

Contents lists available at ScienceDirect

Physics Letters A

www.elsevier.com/locate/pla

Impurity doping effects on the orbital thermodynamic properties of hydrogenated graphene, graphane, in Harrison model

Mohsen Yarmohammadi

Young Researchers and Elite Club, Kermanshah Branch, Islamic Azad University, Kermanshah, Iran

ARTICLE INFO

Article history:
Received 25 May 2016
Received in revised form 28 August 2016
Accepted 16 September 2016
Available online xxxx
Communicated by R. Wu

Keywords:
Graphane
Harrison model
Electronic heat capacity
Magnetic susceptibility
Impurity

ABSTRACT

Using the Harrison model and Green's function technique, impurity doping effects on the orbital density of states (DOS), electronic heat capacity (EHC) and magnetic susceptibility (MS) of a monolayer hydrogenated graphene, chair-like graphane, are investigated. The effect of scattering between electrons and dilute charged impurities is discussed in terms of the self-consistent Born approximation. Our results show that the graphane is a semiconductor and its band gap decreases with impurity. As a remarkable point, comparatively EHC reaches almost linearly to Schottky anomaly and does not change at low temperatures in the presence of impurities. Generally, the total EHC and MS increases with impurity doping. Surprisingly, impurity doping only affect the salient behavior of p_y orbital contribution of carbon atoms due to the symmetry breaking.

1. Introduction

Graphene as a semimetal has a linear band structure near the Dirac points of the Brillouin zone. It was first isolated in 2004 [1] as a weird material because of its unique band structure. Graphene is a single atomic layer with honeycomb lattice including two interpenetrating triangular sublattices C_1 and C_2, as shown in Fig. 1. Graphene has attracted so much attentions both theoretically and experimentally because of its possible applications in nanoscale electronics and optoelectronics [1–9]. In graphene, conductance electrons are from π bonding of p_z orbitals and C_1 and C_2 atoms are joined by covalent, σ, bonding of s, p_x and p_y orbitals. Therefore, in graphene hybridization is sp^2. Graphene is gapless and this creates a problem for using in the electronic devices [10,11]. The band gap is a measurement of the threshold voltage and on-off ratio of the field effect transistors [12,13]. It is desirable to have band gap in materials in addition to their novel features. Theoretically, a fully hydrogenated graphene realized in 2007 [14] and also experimentally predicted in 2009 [15]. They have been found that in the new graphene-like 2D-material, hydrogenated graphene, called *graphane* with sp^3 covalent bonds, carbon atoms react with hydrogen (H) atoms which opens a band gap about 3.5 eV in graphene, making graphene for using such a highly motivated new material in carbon-based nanoelectronics. In graphane, the p_z orbitals of carbon atoms are saturated with hydrogen atoms. Two kinds of graphane is observed, chair-like and boat-like which here we consider chair-like graphane for our investigations.

Recently, several works has been done to compare the thermal properties including thermal conductivity and temperature dependence of EHC of low-dimensional systems with macroscale ones [16–19]. Graphene as the best thermal conductor in nature is the result of Balandin paper in 2011 [17]. Furthermore, the change in orbitals hybridization of atoms can be changed the electronic properties of material which this affects the other properties such as thermal and magnetic indices. By changing the hybridization from sp^2 to sp^3, from graphene to graphane, the dynamics of lattice

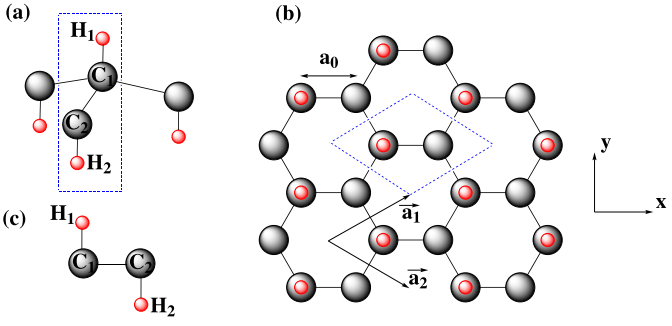

Fig. 1. (a) Schematic diagram of unit cell of chair-like graphane. (b) Top view of chair-like graphane sheet which the dashed lines illustrate the Bravais lattice unit cell. The primitive vectors are denoted by $\vec{a}_1$ and $\vec{a}_2$, while a_0 is the inter-atomic distance. (c) Side view of the system.

E-mail address: m.yarmohammadi69@gmail.com.

http://dx.doi.org/10.1016/j.physleta.2016.09.021
0375-9601/

changes. As an example, Neek-Amal and Rajabpour are calculated the thermal contraction and heat capacity of graphane and introduce a significant Kapitza thermal resistance [20,21]. It is necessary to mention that the thermal properties of a material may find applications in thermal management and thermoelectric [22–26]. Since all nanoelectronic applications are closely related to the thermal properties, the investigation of the thermodynamic properties is important [27]. The EHC of a system is defined as the ratio of that portion of the heat used by the carriers (here, Dirac fermions) to the rise in temperature of the system. On the other hand, MS is the degree of magnetization of a material in response to an applied magnetic field. Many works has been done to study the MS of diverse carbon allotropes [28–38].

Electrons in a system scatters from impurities with a scattering rate τ. This induces a characteristic energy scale $\hbar/\tau$ in the limit of zero doping, that is, at Dirac points. For this reason, impurities have a strong effect on physical properties of material for its applications in electronic devices [39,40]. Many authors have been shown that the impure graphane can be used in transistor devices due to the decreased band gap. For example, Gharekhanlou et al. [41] reported that graphane materials can be used as bipolar transistor and introduced a 2D p–n junction based on graphane [42]. Savini et al. [43] used p-doped graphane to fabricate a prototype high-T_c electron–phonon superconductor. Here, we consider the randomly impurity doping of foreign atoms on chair-like graphane and investigate the total and orbital DOS, EHC and MS of this impure system. We witness that the band gap decreases with impurity doping which is useful for 2D p–n junctions based on graphane. Tight-binding Harrison model within the self-consistent Born approximation describes the dynamic of carriers. The outline of this paper is as follows: Section 2 describes the Hamiltonian and calculation details. In Sec. 3, we show the total and orbital DOS, EHC and MS of the system under impurity doping and in Sec. 4 the numerical results is explained. Finally, Sec. 5 is the summary of paper.

2. The effective Hamiltonian model

In this section, we present the Harrison model to describe the low-energy dynamic of Dirac fermions on the honeycomb lattice of graphane. In Fig. 1, each unit cell includes 4 atoms: two carbon and two hydrogen atoms. The $2s$, $2p_x$, $2p_y$ and $2p_z$ orbitals of each carbon atom and $1s$ orbital of each hydrogen atom participates in the bonding of sp^3 hybridization. Thus, the Hamiltonian can be written as 10×10 matrix

$$H(\vec{\mathbf{k}})=\begin{pmatrix} H_{11}(\vec{\mathbf{k}}) & H_{12}(\vec{\mathbf{k}}) \\ H_{21}(\vec{\mathbf{k}}) & H_{22}(\vec{\mathbf{k}}) \end{pmatrix} \tag{1}$$

where $H_{21}(\vec{\mathbf{k}})=H_{12}^{\dagger}(\vec{\mathbf{k}})$ and the defined tabular form of $H_{11}(\vec{\mathbf{k}})$ is given by

$$H_{11}(\vec{\mathbf{k}})=\begin{pmatrix} h_{ss}^{C_1C_1} & h_{sp_x}^{C_1C_1} & h_{sp_y}^{C_1C_1} & h_{sp_z}^{C_1C_1} & h_{ss}^{C_1H_1} \\ h_{p_xs}^{C_1C_1} & h_{p_xp_x}^{C_1C_1} & h_{p_xp_y}^{C_1C_1} & h_{p_xp_z}^{C_1C_1} & h_{p_xs}^{C_1H_1} \\ h_{p_ys}^{C_1C_1} & h_{p_yp_x}^{C_1C_1} & h_{p_yp_y}^{C_1C_1} & h_{p_yp_z}^{C_1C_1} & h_{p_ys}^{C_1H_1} \\ h_{p_zs}^{C_1C_1} & h_{p_zp_x}^{C_1C_1} & h_{p_zp_y}^{C_1C_1} & h_{p_zp_z}^{C_1C_1} & h_{p_zs}^{C_1H_1} \\ h_{ss}^{H_1C_1} & h_{sp_x}^{H_1C_1} & h_{sp_y}^{H_1C_1} & h_{sp_z}^{H_1C_1} & h_{ss}^{H_1H_1} \end{pmatrix}, \tag{2}$$

In our calculations, we use the reported amounts as below [44–46] by setting $\hbar=k_B=1$. Also on-site energy of p orbitals are considered as the origin of energy. As a remarkable point, the sign of on-site energy of s orbitals is negative, while for p orbitals can be negative or positive [44,47–49].

$$\begin{aligned}
&h_{ss}^{C_1C_1}=-8.868\ \text{eV}, \qquad h_{sp_x}^{C_1C_1}=h_{sp_y}^{C_1C_1}=h_{sp_z}^{C_1C_1}=0,\\
&h_{ss}^{C_1H_1}=-2.50\ \text{eV},\\
&h_{p_xs}^{C_1C_1}=h_{p_xp_x}^{C_1C_1}=h_{p_xp_y}^{C_1C_1}=h_{p_xp_z}^{C_1C_1}=h_{p_xs}^{C_1H_1}=0,\\
&h_{p_ys}^{C_1C_1}=h_{p_yp_x}^{C_1C_1}=h_{p_yp_y}^{C_1C_1}=h_{p_yp_z}^{C_1C_1}=h_{p_ys}^{C_1H_1}=0,\\
&h_{p_zs}^{C_1C_1}=h_{p_zp_x}^{C_1C_1}=h_{p_zp_y}^{C_1C_1}=h_{p_zp_z}^{C_1C_1}=0, \qquad h_{p_zs}^{C_1H_1}=5.72\ \text{eV},\\
&h_{ss}^{H_1C_1}=-2.50\ \text{eV}, \qquad h_{sp_x}^{H_1C_1}=h_{sp_y}^{H_1C_1}=0,\\
&h_{sp_z}^{H_1C_1}=h_{p_zs}^{C_1H_1}, \qquad h_{ss}^{H_1H_1}=-2.40\ \text{eV}.
\end{aligned} \tag{3}$$

Also the general form of $H_{12}(\vec{\mathbf{k}})$ reads

$$H_{12}(\vec{\mathbf{k}})=\begin{pmatrix} h_{ss}^{C_1C_2} & h_{sp_x}^{C_1C_2} & h_{sp_y}^{C_1C_2} & h_{sp_z}^{C_1C_2} & h_{ss}^{C_1H_2} \\ h_{p_xs}^{C_1C_2} & h_{p_xp_x}^{C_1C_2} & h_{p_xp_y}^{C_1C_2} & h_{p_xp_z}^{C_1C_2} & h_{p_xs}^{C_1H_2} \\ h_{p_ys}^{C_1C_2} & h_{p_yp_x}^{C_1C_2} & h_{p_yp_y}^{C_1C_2} & h_{p_yp_z}^{C_1C_2} & h_{p_ys}^{C_1H_2} \\ h_{p_zs}^{C_1C_2} & h_{p_zp_x}^{C_1C_2} & h_{p_zp_y}^{C_1C_2} & h_{p_zp_z}^{C_1C_2} & h_{p_zs}^{C_1H_2} \\ h_{ss}^{H_1C_2} & h_{sp_x}^{H_1C_2} & h_{sp_y}^{H_1C_2} & h_{sp_z}^{H_1C_2} & h_{ss}^{H_1H_2} \end{pmatrix}, \tag{4}$$

in which [44–46]

$$\begin{aligned}
&h_{ss}^{C_1C_2}=-6.769(1+2\varepsilon(\vec{\mathbf{k}}))\ \text{eV},\\
&h_{sp_x}^{C_1C_2}=-5.580(1-\varepsilon(\vec{\mathbf{k}}))\ \text{eV},\\
&h_{sp_y}^{C_1C_2}=-5.580\gamma(\vec{\mathbf{k}})\ \text{eV}, \qquad h_{sp_z}^{C_1C_2}=h_{ss}^{C_1H_2}=0,\\
&h_{p_xs}^{C_1C_2}=5.580(1-\varepsilon(\vec{\mathbf{k}}))\ \text{eV},\\
&h_{p_xp_x}^{C_1C_2}=(2.031\varepsilon(\vec{\mathbf{k}})-5.037)\ \text{eV},\\
&h_{p_xp_y}^{C_1C_2}=4.035\gamma(\vec{\mathbf{k}})\ \text{eV} \qquad h_{p_xp_z}^{C_1C_2}=h_{p_xs}^{C_1H_2}=0,\\
&h_{p_ys}^{C_1C_2}=5.580\gamma(\vec{\mathbf{k}})\ \text{eV}, \qquad h_{p_yp_x}^{C_1C_2}=4.035\gamma(\vec{\mathbf{k}})\ \text{eV},\\
&h_{p_yp_y}^{C_1C_2}=-(6.039\varepsilon(\vec{\mathbf{k}})-3.033)\ \text{eV} \qquad h_{p_yp_z}^{C_1C_2}=h_{p_ys}^{C_1H_2}=0,\\
&h_{p_zs}^{C_1C_2}=h_{p_zp_x}^{C_1C_2}=h_{p_zp_y}^{C_1C_2}=0, \qquad h_{p_zp_z}^{C_1C_2}=t_{p_zp_z}^{\pi}(1+2\varepsilon(\vec{\mathbf{k}}))\ \text{eV},\\
&h_{p_zs}^{C_1H_2}=0, \qquad h_{ss}^{H_1C_2}=h_{sp_x}^{H_1C_2}=h_{sp_y}^{H_1C_2}=h_{sp_z}^{H_1C_2}=h_{ss}^{H_1H_2}=0.
\end{aligned} \tag{5}$$

with $\varepsilon(\vec{\mathbf{k}})=e^{i\vec{\mathbf{k}}.\vec{\mathbf{R}}_+}\cos(\vec{\mathbf{k}}.\vec{\mathbf{R}}_-)$ and $\gamma(\vec{\mathbf{k}})=i\sqrt{3}e^{i\vec{\mathbf{k}}.\vec{\mathbf{R}}_+}\sin(\vec{\mathbf{k}}.\vec{\mathbf{R}}_-)$ where $\vec{\mathbf{R}}_{\pm}=(\vec{a}_1\pm\vec{a}_2)/2$. According to Fig. 1, the primitive unit cell vectors of honeycomb lattice are given by

$$\vec{a}_1=\frac{a_0}{2}(\sqrt{3}\hat{i}+\hat{j}), \qquad \vec{a}_2=\frac{a_0}{2}(\sqrt{3}\hat{i}-\hat{j}) \tag{6}$$

where $a_0\approx 1.4\ \text{Å}=0.14$ nm is the length of lattice translational vector. Also $\hat{i}$ and $\hat{j}$ are unit vectors along the x and y directions, respectively. The $H_{22}(\vec{\mathbf{k}})$ term is the same with $H_{11}(\vec{\mathbf{k}})$, but $h_{p_zs}^{C_2H_2}=-h_{p_zs}^{C_1H_1}$ and $h_{sp_z}^{H_2C_2}=-h_{sp_z}^{H_1C_1}$ due to the opposite place of H_2 with respect to the graphane plane in the unit cell, as shown in Fig. 1. Since unit cell of graphane includes four atoms, the Green's function can be written as the 4×4 matrix. In the Matsubara formalism [50], each element of the Green's function matrix is defined by

$$\begin{aligned}
&G_{\alpha\beta}(\vec{\mathbf{k}},\gamma)=-\langle T_\gamma c_{k,\alpha}(\gamma)c_{k,\beta}^{\dagger}(0)\rangle\\
&G_{\alpha\beta}(\vec{\mathbf{k}},i\omega_n)=\int_0^{1/k_BT} e^{i\omega_n\gamma}G_{\alpha\beta}(\vec{\mathbf{k}},\gamma)d\gamma
\end{aligned} \tag{7}$$

where T_γ is the time correlation, $c=a(b)$ and α,β refer to each sublattice atoms C_1, C_2 and H_1, H_2 and γ is the imaginary time. Also $\omega_n=(2n+1)\pi k_BT$ is the Fermionic Matsubara's frequency. The Green's function matrix of the system ($\mathbf{G}$) can be readily obtained by the following equation